



Analytical Approach of Brillouin Fiber Amplifier Gain up to 2 km Long Fibers

2 km'ye kadar olan Brillouin Fiber Kuvvetlendiricilerde Kazancın analitik ifadesinin elde edilmesi

Fikri Serdar Gökhan* 

*Department of Electrical and Electronics Engineering, Alanya Alaaddin Keykubat University, Kestel, Alanya, Antalya, TURKEY

Sorumlu Yazar / Corresponding Author *: fsgokhan@gmail.com

Geliş Tarihi / Received: 02.05.2019

Kabul Tarihi / Accepted: 05.08.2019

Araştırma Makalesi/Research Article

DOI: 10.21205/deufmd.2020226416

Atıf şekli/ How to cite: GÖKHAN, S.G. (2020). Analytical Approach of Brillouin Fiber Amplifier Gain up to 2 km Long Fibers . DEUFMD 22(64),159-166.

Abstract

In order to obtain analytical gain expression in Brillouin optical Fiber Amplifiers (BFAs), coupled intensity equations describing the interaction of pump and Stokes waves must be solved simultaneously. For long optical fibers, although fiber loss is responsible for the pump depletion and nonnegligible effect, for short optical fibers less than 2 km, its effect can be discarded. In this paper, we provide an accurate analytic expression for the BFA gain for fiber lengths less than 2 km by discarding the optical fiber loss and show results of experimental validation.

Keywords: Stimulated Brillouin scattering, Coupled Intensity Equations, Brillouin Fiber Amplifiers

Öz

Brillouin Fiber Kuvvetlendirici (BFK) kazancının analitik ifadesini elde etmek için, pompa ve Stokes dalgalarının etkileşimini tanımlayan denklemlerin çözümü gerekmektedir. Uzun optik fiberler için fiber kaybı, pompa lazerini tüketmesi nedeniyle ihmal edilemez bir parametre olmasına rağmen, 2 km'den kısa BFK' de etkisi ihmal edilebilir. Bu makalede, optik fiber kaybı ihmal edilerek, 2 km'den daha kısa optik fiberler için BFK kazancı analitik olarak ifade edilerek, bu ifadenin doğruluğu deneysel olarak gösterilmiştir.

Keywords: Uyarılmış Brillouin Saçılımı, Kuple Brillouin Denklemleri, Brillouin Fiber Kuvvetlendiriciler

1. Introduction

Stimulated Brillouin scattering (SBS) is the most efficient nonlinear amplification mechanism in optical fibers, which can be initiated by launching a small amount of optical power at the Stokes frequency from the opposite end of the fiber [1]. SBS can be used to amplify a weak signal whose frequency is shifted from the

pump frequency by an amount equal to the Brillouin shift when the weak signal (seed Stokes wave) is input from the rear (opposite to the pump) end of the fiber. This has led to the design of (BFA) and has been implemented in a wide range of applications, such as an active filter due to its narrowband amplification feature [2] or in the control of pulse propagation in optical fibers [3]. The BFA can

also be used to measure strain and temperature [4] which has led to the design of distributed Brillouin sensors (DBS). In these type of sensors, strain and temperature can be measured along the whole fiber length [5]. In the BFA configuration, SBS can be used for efficient narrow band amplification when the Stokes wave is input from the rear (opposite to the pump) end of the fiber.

Interaction between the pump and the Stokes wave due to SBS is described by a system of ordinary differential equations (ODEs) [6]. The system of ODEs for BFAs has well-defined boundary conditions: $P_p(0) = P_0$ and $P_s(L) = P_{Stokes}$. Such a mathematical problem is known as the two-point boundary value problem. Since the boundary value of the $P_p(L)$ and/or $P_s(0)$, with L being the fiber length, is undetermined, such systems of non-linear ODEs is typically addressed numerically. The exact analytical solution to the system of ODEs is known only for lossless medium with the exception of an analytical solution of integration constant C and obtained expression is a transcendental equation giving the unknown quantity $P_s(0)/P_p(0)$ in terms of the known quantities $P_p(0)$ and $P_s(L)$ [7-8]. On the other hand, the contribution of loss is a very important effect in optical fibers because the pump-Stokes interaction occurs over long distances and both the pump and the Stokes waves can be attenuated by orders of magnitude. For example, on propagation in a 50 km-long standard single-mode optical fiber, the input power is reduced to a level of 10% from its original value due to the attenuation of the fiber. However for 1 km and 2 km fiber lengths, this ratio is increased to %95.5 and %91, respectively. Therefore, for 2 km and 1 km long fiber, pump depletion due to the fiber attenuation is around %9 and %4.5 respectively. Thus approximately up to 2 km fiber lengths, the error in prediction of the gain of BFA when discarding the fiber attenuation is negligible.

In this paper, we focus on the derivation of the conserved quantity (integration constant) c using asymptotic theory [9]. Depending on this quantity, analytical prediction of pump, Stokes evolution, the gain and the working range of the amplifier is obtained. While concentrating this derivation, we assume that the fiber length is up to 2 km and attenuation of the fiber is

negligible. On the other hand, the saturation conditions of the BFA is derived for this limited length. The derived approximate analytical solution will be the solution of topic *Pump Depletion Effects in SBS* aforementioned in Ref. [7]

2. Material and Method

The coupled ODEs for the evolution of the intensities of pump I_p and Stokes I_s can be written as [10,11,12]

$$\frac{dI_p}{dz} = -g_B I_p I_s - \alpha I_p \quad (1a-1)$$

$$\frac{dI_s}{dz} = -g_B I_p I_s + \alpha I_s \quad (1a-2)$$

here $0 \leq z \leq L$ is the propagation distance along the optical fiber of the total length L , g_B is the Brillouin gain coefficient and α is the fiber loss coefficient. Note that, here we assume a Stokes wave launched from the rear end of the fiber. Then the known values of the input pump intensity $I_p(0) = I_{p0}$ and the input Stokes intensity $I_s(L) = I_{sL}$ are the boundary values. When the fiber loss is negligible, i.e., up to 2km fiber length, Eq.(1a) will be;

$$\frac{dI_p}{dz} = -g_B I_p I_s \quad (1b-1)$$

$$\frac{dI_s}{dz} = -g_B I_p I_s \quad (1b-2)$$

The geometry of an SBS amplifier is shown in Figure 1.

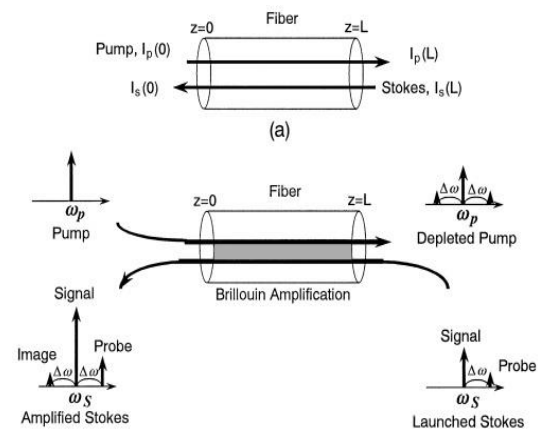


Figure 1. Geometry of an SBS amplifier.

The solution of (1b-1,1b-2) leads to [13],

$$I_p(z) = c I_{p0} [I_{p0} + (c - I_{p0}) \exp(-c g_B z)]^{-1} \quad (2a)$$

$$I_s(z) = c (I_{p0} - c) [I_{p0} \exp(c g_B z) + (c - I_{p0})]^{-1} \quad (2b)$$

where,

$$I_p(z) = I_s(z) + I_{p0} - I_{s0} \quad (3a)$$

$$c = I_p(z) - I_s(z) = I_{p0} - I_{s0} \quad (3b)$$

c is the conserved quantity.

To explicitly find the value of parameter c we approximately solve the equation:

$$I_{sL} = c (I_{p0} - c) [I_{p0} \exp(c g_B L) + (c - I_{p0})]^{-1} \quad (4)$$

using boundary condition I_{sL} . Within the paper, we will show two different solutions to the c depending on the High Gain Region (c_1) and Saturation region (c_2).

2.1. Solution of c for High-Gain Region

In this region, the solution of ($c = c_1$) becomes,

$$c_1 \approx \frac{1}{\kappa} \left\{ \Lambda + \ln \left(\Lambda \left(1 - \frac{\Lambda}{\kappa} \right) \right) - \ln \left(1 - \frac{1}{e^\Lambda} \right) - \ln \left(1 + \frac{\Lambda}{\kappa(e^\Lambda - 1)} \right) \right\} \cdot I_{p0} \quad (5)$$

where $\varepsilon = \frac{I_{sL}}{I_{p0}}$, $\kappa = g_B I_{p0} L$ and $\Lambda = -\ln(\varepsilon \kappa)$. In [Fig.2], the comparison of Eq. (5) with the numerical solution is made. A very good agreement between predictions of the analytical formula of c_1 and the numerical solution can be seen. From the figure, it can be inferred that when ε decreases, the accuracy of c_1 increases.

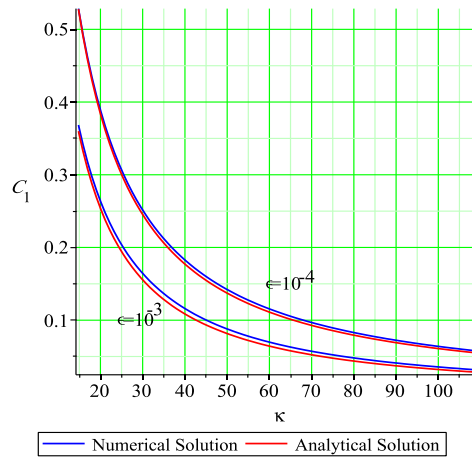


Figure 2. The comparison of prediction of Eq.(5) with the numerical solution of Eq.(4). Parameters: $A_{eff} = 80 \mu m^2$, $g_B = 1.091 \times 10^{-11} [m/W]$

The BFA in the high gain region up to 2 km can be calculated from the approximation in (2b), and expressed in terms of the physical parameters as;

$$G_{High-Gain} = \frac{P_s(0)}{P_s(L)} \approx \frac{(P_{p0} - c_1 A_{eff})}{P_{sL}} \quad (6)$$

2.2. Solution of c for Saturation Region

In this case, the solution of ($c = c_2$) can be analytically defined as,

$$c_2 \approx -0.99 I_{sL} - \frac{1}{g_B L} \text{LambertW}(-I_{sL} g_B L \cdot \exp(-0.99 I_{sL} g_B L)) \quad (7)$$

where LambertW is a function which satisfies $\text{LambertW}(x) \exp(\text{LambertW}(x)) = x$. The BFA gain in saturation can be calculated using Eq.(7) and expressed as;

$$G_{Saturate} = \frac{P_s(0)}{P_s(L)} \approx \frac{(P_{p0} - c_2 A_{eff})}{P_{sL}} \quad (8)$$

3. Results

In the experimental setup adopted in Ref. [14] (Fig. 3), External Cavity Laser (ECL) with output power 40 mW, linewidth smaller than 50 kHz and $\lambda_p = 1550$ nm is split into pump and probe channels. In the pump side, laser was used together with an EDFA to generate up to 70 mW of pump power. In the probe side, the Stokes wave was obtained using a Mach-Zehnder modulator (MZM). The electrical spectrum analyzer was used to determine the Brillouin frequency shift (ν_B) of the fiber and, correspondingly, the modulation frequency for the MZM (10.877 GHz for standard single-mode fiber). A fiber Bragg grating in the reflecting regime was used to select a sideband of the MZM output. A Stokes-shifted probe is selected by Fiber Bragg Grating (FBG). A polarization scrambler and isolator are also utilized before launching the probe signal into the Fiber Under Test (FUT), which is a standard single-mode fiber (Corning® SMF-28e® Fiber, ITU G.652 compliant). The polarization scrambler averages out the polarization dependence on the Brillouin gain, while the isolator avoids the interference of pump in MZM. The polarization controller placed at the output of the laser was used to maximize the detected power.

Powermeters were used to monitor the input pump power P_{p0} , the transmitted pump power P_{pL} , the launched seed power P_{sL} , and the amplified Stokes power P_{s0} . To keep the attenuation low as possible, maximum 2 km fiber length was experimentally studied.

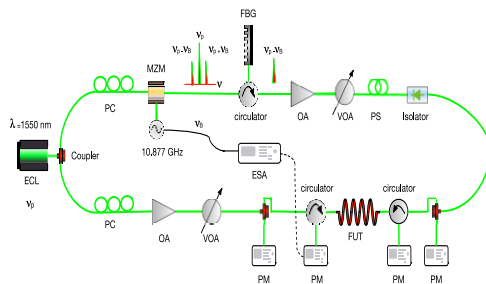


Figure 3. Experimental setup for BFA measurements: ECL, External Cavity Laser, PC, polarization controller; MZM, Mach-Zehnder modulator; FBG, fiber Bragg grating; OA, optical amplifier; VOA, variable optical attenuator; PS, polarization scrambler; PM, powermeter; ESA,

electrical spectrum analyzer and FUT, fiber under test.

Here, the key parameter γ (the gain parameter corresponding to the dominant acoustic mode, nonlinear coefficient measured in $\text{m}^{-1}\text{W}^{-1}$) inherently involves polarization effects. γ depends on:

$$\gamma = \frac{g_B}{KA_{ao} \left(1 + \frac{\omega_{las}}{\omega_B}\right)} \quad (9)$$

where, g_B is the peak Brillouin gain of the dominant acoustic mode, A_{ao} account for acousto-optic effective area; K and $\left(1 + \frac{\omega_{las}}{\omega_B}\right)$ account for polarization effects and the finite spectral line width of the input signal, respectively.

Nonlinear parameter γ is different for different types of the fibers (see: Table 1, in Ref[6]). γ mainly depends on A_{ao} . Unlike the optical effective area A_{eff} and conventionally used to describe SBS in optical fibers, A_{ao} actually determines the total Brillouin gain. The fiber types, with different index profile, and dopant types, have different A_{ao} acousto-optic effective area that is not same with the optical effective area (A_{eff}). It is approximately same for fiber profiles that are close to step index. (This explains why approximating A_{ao} with A_{eff} gives good agreement with experimental data when step-index, standard single-mode fibers are used) However, for nonuniform fiber profiles, the parameter A_{ao} rather than A_{eff} determines the strength of the acousto-optic interaction and is responsible for different SBS thresholds in optical fibers with different index profiles. Therefore A_{ao} rather than A_{eff} have to be known prior to computation, while it can be only known during measurement.

γ also depends on the polarization of the pump. If full scrambler is used $K= 3/2$ differs from 2. On the other hand laser spectral bandwidth should be low as possible. The spectral bandwidth of the laser source should be less than 100 KHz and in the range of Brillouin linewidth ω_B . The Brillouin linewidth is around 20 MHz for the standard single-mode fiber

We have used non-PM fiber. We have used typical standard single mode fiber (Corning® SMF-28e® Fiber, ITU G.652 compliant) as a Fiber Under Test. For typical (step-index, with a quasi-rectangular index profile) standard single-mode fibers and for the *full polarization scrambling*, it is $\gamma = 0.14 \text{ (m}^{-1}\text{W}^{-1}\text{)}$ (see: Table 1, in Ref[6]).

If specific values of the used fiber type (FUT-fiber under test), polarization type, and laser spectral width, A_{ao} , γ can be best determined by the numerical fit of the transmitted pump power (P_{pL}) versus input pump power [Fig(4a)] for the different polarization effects and for different fiber types. In our experiment we determined $\gamma = 0.138 \text{ m}^{-1}\text{W}^{-1}$ and it is very close to $0.14 \text{ m}^{-1}\text{W}^{-1}$ reported by the Andrey Kobayakov et. al.

On the other hand, if polarization scrambler is not used γ will be around $\gamma \approx 0.1 \text{ m}^{-1}\text{W}^{-1}$ (Because K would be around 2 instead of 1.5). On the other hand, If Polarization Maintaining (PM) is used, γ will be around $\gamma \approx 0.21 \text{ m}^{-1}\text{W}^{-1}$ (Because K would be around 1 instead of 1.5). But exact values can be only determined by the test setup.

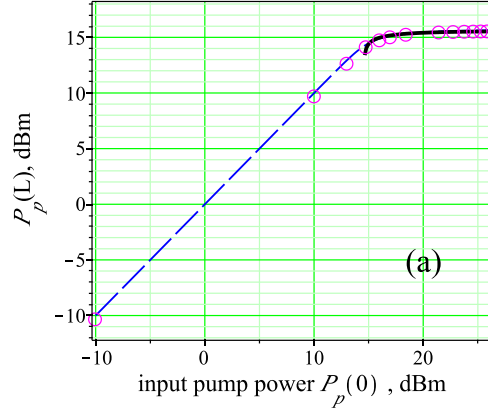
The experimental results are plotted in [Fig. 4] together with theoretical predictions. We find a high level of agreement for the transmitted pump for all input pump levels above critical pump power [Fig. 4(a)]. As for the amplifier gain G_{BFA} , we find an excellent agreement between predictions of Eq.(6) and the experimental data [Fig. 4(b)]. We note that Eq.(6) is applicable only when the pump power exceeds the critical value, $P_{p0} > P_{cr} \approx \frac{\Lambda + \sqrt{\Lambda^2 + 4\Lambda}}{2\gamma L}$

where γ is nonlinear constant and its value is around $0.14 \text{ W}^{-1}\text{m}^{-1}$. Below this critical power (weak-pump regime), since $|g_B I_p I_s| \ll |\alpha I_p|$, the effect of attenuation is still effective [Fig. 4(c)]. Thus, *Undepleted Pump Approximation* (UPA) for the BFA gain is applicable and it is,

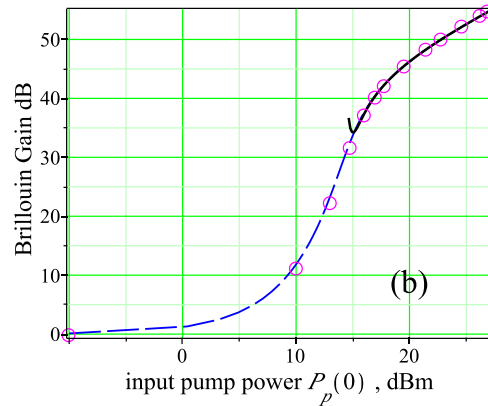
$$G_{UPA} = \exp\left(g_B P_{p0} \frac{L_{eff}}{A_{eff}} - \alpha L\right) \quad (10)$$

The trend of numerical and experimental data below critical pump power follows Eq.(10) which includes attenuation term, although we try to discard it. This outcome explains why

UPA solution is important and used as a general case.



○ Experimental data
 - - Numerical Solution
 — Proposed Solution for High Gain Region with c_1



○ Experimental data
 - - Experimental Results
 — Proposed Gain for High Gain Region with c_1

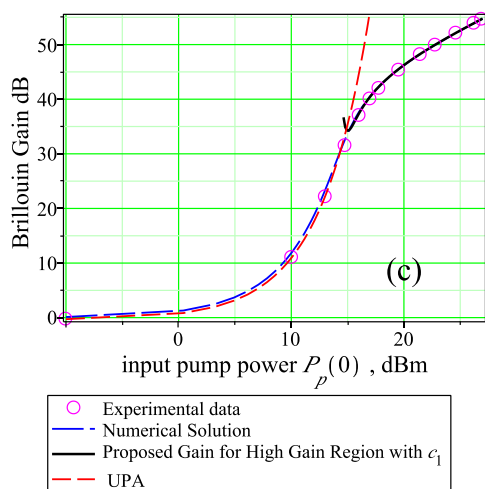


Figure 4. (a) Transmitted pump power $P_p(L)$ and (b) BFA gain in high-gain region versus input pump power $P_p(0)$. (c) Insertion of UPA Gain below critical pump power in (b). Open circles, experimental data; thick solid line, prediction of Eq. (6); long dashed line, numerical result, dashed line prediction of UPA. Parameters in all figures: $L = 2 \text{ km}$, $P_{sL} = 1.55 \mu\text{W}$, $A_{eff} = 80 \mu\text{m}^2$, $g_B = 1.091 \times 10^{-11} \text{ [m/W]}$

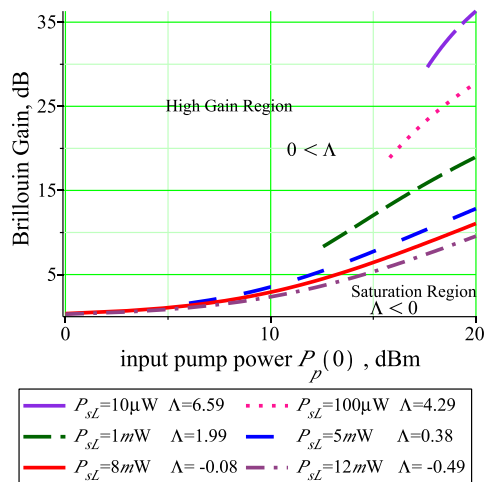
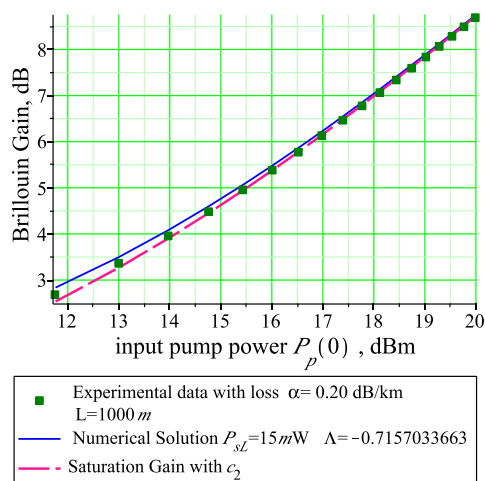


Figure 5. The Brillouin gain pattern of High-gain and Saturation region for different P_{sL} Stokes powers. $L = 1 \text{ km}$, $A_{eff} = 80 \mu\text{m}^2$, $g_B = 1.091 \times 10^{-11} \text{ [m/W]}$

In [Fig. 5], Brillouin Gain obtained with the numerical solution of Eq.(1b) is plotted with the respective P_{sL} and Λ values. It can be inferred from the figure that the sign of Λ is opposite in High-Gain and Saturation Regime. In High-Gain region while $\Lambda > 0$, $P_{sL} < \frac{1}{g_{BL}}$ in Saturation region $\Lambda < 0$, $P_{sL} > \frac{1}{g_{BL}}$. Clearly $\Lambda = 0$ is a border between two regions. It must be noted that, aforementioned applications in Ref.[2-5] typically require pump powers above SBS threshold and exploits High-Gain and Saturation region. In Fig 6, BFA gain in the Saturation Region is compared with the experimental data. In the experiment, standard single-mode fiber with the attenuation factor $\alpha=0.2 \text{ dB/km}=0.046 \text{ [1/km]}$ is used. From the figure, we find a high level of agreement between predictions of gain computed with Eq.(8) and the measured gain. It can be concluded that agreement between the saturation gain in Eq.[8] with the measurement fits well if the fiber length is increased.



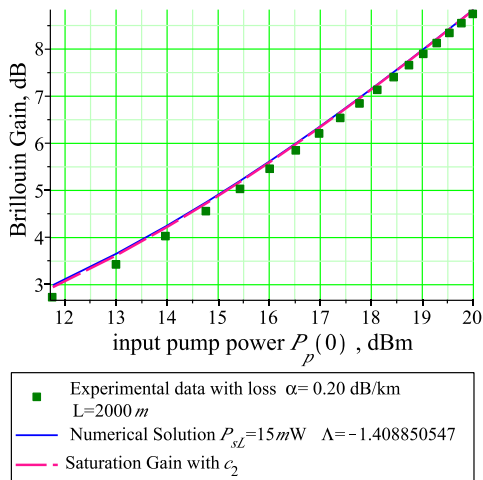


Figure 6. Comparison of Eq.[8] with experimental data in the Saturation Region. Dashed Line represent predictions of the Eq.[8], Diamond represent Experimental Data and Solid curves represent Numerical Solution. Parameters: a) $L = 1 \text{ km}$ and b) $L = 2 \text{ km}$, other parameters are $P_{SL} = 15 \text{ mW}$, $A_{eff} = 80 \mu\text{m}^2$, $g_B = 1.091 \times 10^{-11} \text{ [m/W]}$

4. Discussion and Conclusion

We have presented an approximate analytical solutions to the system of SBS equations in a lossless medium in three different regimes, namely, weak-pump, high gain and saturation regions. The limits of the three separation conditions are determined and the respective BFA gain to these regions are accurately defined. Especially, for the lossless medium, the gain approximation of BFA for the high-gain and saturation region, is introduced for the first time to our best of knowledge. The results obtained can be practically used to optimize performance of Brillouin fiber amplifiers for fiber lengths up to 2 km.

In Table 1, the usage of the equations described so far is briefly listed. Eq.(6) is valid in the high-gain region where the pump power should be more than the P_{cr} . Eq.(10) is valid in the weak-pump region where Undepleted pump approximation (UPA) is accurate enough to predict BFA gain and in this region, P_{p0} should be less than P_{cr} . For the saturation region the

condition is $\Lambda < 0$ or $P_{SL} > \frac{1}{g_B L}$ and Eq.(8) can be used to predict the BFA gain.

Table 1. Brief usage of the Equations.

Criteria	Region	Gain Equation
$P_{p0} < P_{cr} \approx \frac{\Lambda + \sqrt{\Lambda^2 + 4\Lambda}}{2\gamma L}$	Weak-pump	(10)
$P_{p0} > P_{cr} \approx \frac{\Lambda + \sqrt{\Lambda^2 + 4\Lambda}}{2\gamma L}$	High-Gain Region	(6)
$P_{SL} > \frac{1}{g_B L}$	Saturation Region	(8)

References

- [1] Olsson, N. A., Van der Ziel, J. P. 1986. Cancellation of fiber loss by semiconductor laser pumped Brillouin amplification at 1.5 μm : Applied Physics Letters, vol. 48, p. 1329–1330. DOI: 10.1063/1.96950
- [2] Tkach, R. W., Chraplyvy, A. R. and Derosier, R. M. 1989. Performance of a WDM network based on stimulated Brillouin scattering: IEEE Photonics Technology Letters, vol.1, pp. 111–113. DOI: 10.1109/68.34758
- [3] Song, K. Y., Herráez, M. G., and Thévenaz, L. 2005 Observation of pulse delaying and advancement in optical fibers using stimulated Brillouin scattering: Optics Express, vol. 13, pp. 82–88. DOI: 10.1364/OPEX.13.000082
- [4] Culverhouse, D. Frahi, F. Pannell, C. N. and Jackson, D. A. 1989. Potential of stimulated Brillouin scattering as sensing mechanism for distributed temperature sensor: Electronics Letters. vol. 25, pp. 913–915. DOI: 10.1049/el:19890612
- [5] Gokhan, F. S. 2011. Moderate-gain Brillouin amplification: an analytical solution below pump threshold: Optics Communications, vol. 284, pp. 4869–4873. DOI: 10.1016/j.optcom.2011.06.054
- [6] Kobayakov, A. Sauer, M. and Chowdhury, D. 2010. Stimulated Brillouin scattering in optical fibers: Advances in Optics and Photonics, vol. 2, pp. 1–59. DOI: 10.1364/AOP.2.000001
- [7] Boyd, R.W. 2007. Nonlinear Optics, 3rd edition. Academic Press, Rochester, New York, chap.9. pp. 442–443
- [8] Zel'dovich, B. Ya., Pilipetsky, N. F. and Shkunov, V. V. (Springer-Verlag, 1985). Principles of Phase Conjugation. chap. 2.
- [9] Daniel Richardson, Bruno Salvy, John Shackell, Joris Van Der Hoeven. 1996. Asymptotic Expansions of exp-log Functions. [Research Report] RR-2859, INRIA.
- [10] Agrawal, G. P. 2001. Nonlinear Fiber Optics, 3rd edition, Academic Press, New York, chap.9. pp. 360
- [11] Boyd, R.W. 2007. Nonlinear Optics, 3rd edition. Academic Press, Rochester, New York, Chap.9. pp. 463

- [12] Chen, L. and Bao, X. 1998. Analytical and numerical solutions for steady state stimulated Brillouin scattering in a single-mode fiber: Optics Communications, vol. 152, pp. 65-70. DOI: 10.1016/S0030-4018(98)00147-3
- [13] Gökhan, F. S., Gökteş, H. and Sorger, V. J. 2018. Analytical approach of Brillouin amplification over threshold: Applied Optics, vol. 57, pp. 607-611. DOI: 10.1364/AO.57.000607
- [14] Gökhan, F. S., Gökteş, H. 2019. Analytical approach to calculate the gain of Brillouin fiber amplifiers in the regime of pump depletion: Applied Optics, vol. 58, pp. 7628-7635. DOI: 10.1364/AO.58.007628